Geophysical Research Letters

RESEARCH LETTER
10.1029/2019GL084180

Key Points:
- Across the globe, physical weathering mobilizes highly bioavailable iron that reaches the oceans as dust and sediments
- Chemically weathered regions supply iron to the ocean that is generally less bioavailable than that from physically weathered regions
- Relative rates of physical and chemical weathering likely influence the biological pump as well as the abiotic silicate-carbonate cycle

Supporting Information:
- Supporting Information S1

Correspondence to:
E. M. Shoenfelt,
shoen@mit.edu

Citation:
Shoenfelt, E. M., Winckler, G., Annett, A. L., Hendry, K. R., & Bostick, B. C. (2019). Physical weathering intensity controls bioavailable primary iron (II) silicate content in major global dust sources. *Geophysical Research Letters*, *46*, 10,854–10,864. https://doi.org/10.1029/2019GL084180

Received 19 JUN 2019
Accepted 3 SEP 2019
Accepted article online 11 SEP 2019
Published online 10 OCT 2019

Physical Weathering Intensity Controls Bioavailable Primary Iron(II) Silicate Content in Major Global Dust Sources

Elizabeth M. Shoenfelt[1,2,3], Gisela Winckler[1,2], Amber L. Annett[4], Katharine R. Hendry[5], and Benjamin C. Bostick[2]

[1]Department of Earth and Environmental Sciences, Columbia University, New York, NY, USA, [2]Lamont-Doherty Earth Observatory, Palisades, NY, USA, [3]Now at Department of Earth, Atmospheric and Planetary Sciences, Massachusetts Institute of Technology, Cambridge, MA, USA, [4]School of Ocean and Earth Science, University of Southampton, Southampton, UK, [5]School of Earth Sciences, University of Bristol, Bristol, UK

Abstract The speciation of iron (Fe) reaching the ocean, for instance in wind-blown dust and coastal sediments, impacts its bioavailability to phytoplankton and its impact on atmospheric carbon dioxide (CO_2) and climate. For dust reaching the Southern Ocean, primary Fe(II) silicates that are physically weathered from bedrock are highly bioavailable compared to more chemically weathered, Fe(III)-rich species, suggesting that weathering in dust source regions impacts the bioavailable Fe supply. However, this phenomenon has not been studied in other important terrestrial Fe sources, where weathering regimes and source geology vary. Here, we use Fe X-ray absorption spectroscopy on marine sediment cores to show that major global dust and sediment sources impacted by high physical weathering contain abundant primary minerals and thus are overlooked as a source of highly bioavailable Fe globally. Thus, it is important to consider the role of physical versus chemical weathering in Fe fertilization and biotic CO_2 cycling.

Plain Language Summary Iron is an important trace metal nutrient that is necessary for all life. In many regions of the ocean, terrestrial dust and sediment are important iron sources to living things, especially photosynthetic organisms that can lower atmospheric CO_2 and global temperatures over time. For an important dust source in the iron-limited Southern Ocean, the chemical form of iron controls how well it is utilized by organisms; the iron contained in fresh bedrock minerals is more bioavailable than iron that has been exposed for longer periods on land and has turned to rust. Thus, the physical weathering of bedrock by glaciers has been shown to mobilize highly bioavailable iron that likely fertilizes phytoplankton, but we do not know whether physical weathering by other mechanisms in other parts of the globe influences iron bioavailability. Here we show that physical mobilization of primary minerals increases the bioavailable iron content of other major dust and sediment sources, and we confirm that regions dominated by chemical rather than physical weathering do not contribute sediments with significant amounts of highly bioavailable iron.

1. Introduction

Iron (Fe) is a micronutrient that is essential for all marine life (Sunda et al., 2005). In oxygenated seawater, dissolved Fe rapidly precipitates as ferrihydrite (Sunda, 2001), making terrestrial dust an important source of new Fe to phytoplankton in many regions of the ocean (Boyd & Ellwood, 2010). In high-nutrient low-chlorophyll upwelling regions, where bioavailable Fe supply limits phytoplankton growth, dust-borne Fe transported over long distances is a significant source of Fe to the remote region where riverine and shelf sediment Fe is minimal (Martínez-García et al., 2014). In the low-nutrient, downwelling gyre regions, some phytoplankton have high Fe demands due to the role of Fe in nitrogen fixation, and these phytoplankton have been shown to mobilize solid-phase Fe from natural inputs of Saharan dust to fulfill their needs (Polyviou et al., 2018; Rubin et al., 2011). Global dust fluxes modulate climate in part through phytoplankton fertilization feedbacks (Schepanksi, 2018). For instance, dust-borne Fe fertilization of subantarctic Southern Ocean phytoplankton has been associated with about half of the CO_2 drawdown in the last glacial cycle (Martínez-García et al., 2014).

When estimating the bioavailable Fe supply that can promote phytoplankton growth, all sediment Fe is not equal. The Fe associated with glaciogenic primary Fe(II) silicates is highly labile and bioavailable to diatoms

compared to that associated with nonglaciogenic Fe(III) oxides and secondary minerals (Shoenfelt et al., 2017), as supported by high Fe solubility in glacial versus nonglacial Fe sources (Hawkings et al., 2018; Schroth et al., 2009). The difference in Fe bioavailability between glaciogenic and nonglacigenic Fe-bearing sediments likely impacts nutrient regimes over glacial-interglacial cycles. The dust-borne Fe speciation record over the last glacial cycle in the subantarctic Southern Ocean shows that the fraction of bioavailable glacial Fe positively correlates with total Fe flux and suggests that physical weathering by glaciers is likely more important to Southern Ocean dust fluxes and Fe fertilization than previously recognized (Shoenfelt et al., 2018). However, we do not know whether the source geology and degree of physical weathering in major dust regions control dust-borne Fe speciation and bioavailability globally.

The mechanical alteration of bedrock is an important prerequisite to dust production in a given region. Physical weathering mobilizes minerals from bedrock without affecting their mineralogy by breaking source rock into smaller grains. In general, physical weathering is most significant in places where soil development and plant cover are low, through mechanical action by ice, rocks embedded in ice, rocks carried by rivers, and rocks falling down high slopes (Weaver, 1990). Rates of physical weathering generally increase with (1) increased glacial activity of continental glaciers at the poles and (2) faster fluvial and gravitational weathering due to steep slopes that result from mountain building (Anderson, 2005; Riebe et al., 2004; Scher & Bohaty, 2011). Physical weathering exposes rocks under continental glaciers and in uplifted mountains that often contain highly bioavailable primary Fe(II) aluminosilicates ("Fe(II) silicates") from igneous and metamorphic mafic (Fe rich) rocks (Herman et al., 2015; Kalsbeek, 1982; Montgomery et al., 2001).

Chemical weathering results in the conversion of primary Fe(II) silicates that form in bedrock due to high temperature and low oxygen fugacity (e.g., olivine, pyroxene, amphibole, and biotite) to secondary Fe(III) oxides and clay minerals (Bowen, 1922; Carmichael & Ghiorso, 1986; Cornell & Schwertmann, 2003; Sposito, 2008). The chemical weathering of primary iron-bearing minerals is usually rapid, since primary minerals are far from equilibrium with surface conditions (Bowen, 1922), and these rates increase with higher temperatures and precipitation (Sposito, 2008). Solid-phase Fe is transferred from a range of source areas to the ocean though riverine transport of sediment, sea ice transport of various particles, and eolian transport of dust, of which eolian transport of dust is most important to remote open-ocean regions (Martínez-García et al., 2014). Eolian processes are often assumed to transport secondary Fe(III)-rich aluminosilicates and oxidized Fe(III) particles that are the products of chemical weathering, given the mineralogical composition of major low-latitude dust sources (Hawkings et al., 2018; Raiswell et al., 2008; Rodriguez-Navarro et al., 2018; Shi et al., 2012). However, both solid-phase Fe(II) and Fe(III) species exist in the surface ocean (von der Heyden et al., 2012), and continental margins can supply primary Fe(II) silicates to the oceans through physical weathering of bedrock (Lam et al., 2012). High rates of physical weathering at the poles result in primary, terrestrial chlorite minerals dominating the clay-size fraction of polar marine sediments (Griffin et al., 1968). Since chlorite and other primary minerals rapidly chemically weather, the existence of this mineral in marine sediments is evidence of cold and dry conditions, where glacial physical weathering is high and chemical weathering is low (Ehrmann et al., 1992; Winkler et al., 2002). The high abundance of similar primary minerals in glacial dust sources (Shoenfelt et al., 2017) and glacial dust reaching the Southern Ocean (Shoenfelt et al., 2018) suggests that they may be more common than previously recognized in eolian and other sediment transported to the ocean. Since primary minerals in glacial sediments are associated with Fe fertilization of phytoplankton (Shoenfelt et al., 2017; Shoenfelt et al., 2018), physical weathering may be directly coupled to ocean biogeochemistry and climate. Ongoing research is investigating the precise mechanism by which the Fe associated with Fe(II) silicates is bioavailable to phytoplankton, including the possibilities that freshly exposed reactive surfaces and fresh ferrihydrite intermediates contribute to bioavailability and uptake rates. If different Fe minerals and Fe uptake regimes dominate in low-latitude versus high-latitude ocean regions, this may explain how different phytoplankton species interact with different dust-borne Fe minerals (Polyviou et al., 2018; Rubin et al., 2011).

Here, we investigate the global role of source region geology and weathering extent on particulate Fe speciation and bioavailability, by probing the Fe speciation in a collection of four marine sediment cores impacted by physically weathered sediments: Labrador sea core tops impacted by sediments mobilized by the Greenland ice sheet; subantarctic South Atlantic and South Pacific cores impacted by South American and New Zealand/Australian glaciogenic and nonglaciogenic dust; and a North Pacific core impacted by East Asian dust composed in part of sediments mobilized from mountains adjacent to the desert dust

source regions. We compare these physical-weathering-impacted cores with one low-latitude core free of glacial influence or significant fluvial or other physical weathering processes promoted by steep mountain slopes: a West African Margin core impacted by Saharan dust.

We use Fe K-edge X-ray absorption spectroscopy (XAS) to determine the contribution of Fe(II) silicate minerals to total particulate Fe, following Shoenfelt et al. (2017, 2018). With this method, we can characterize just the Fe-rich minerals in the bulk sediments. We use principal component analysis (PCA) to characterize key features in the X-ray absorption spectra and isolate the impact of key primary and secondary minerals on the observed differences between glaciogenic and nonglaciogenic sediments. The Fe speciation data can tell us the importance of primary versus secondary minerals in the Fe fraction, to investigate the global role of highly bioavailable Fe in primary minerals from areas with high physical weathering and less bioavailable Fe in secondary minerals from areas with high chemical weathering.

2. Materials and Methods

2.1. Sediment Sampling

A map of the five marine sediment core locations shows the global scope of this study (Figure S1 in the supporting information). The Greenland core top samples were filtered from ~5 or ~15 cm of overlying core-top water from megacores recovered from the bottom of the Labrador Sea and include suspended particles in bottom water as well as core-top sediment resuspended by the recovery process. Latitudes, longitudes, depths, and approximate distance from the Greenland shoreline for the four samples are (1) 60.2618°N, 46.89084°W, 572 m, ~50 km; (2) 59.394973°N, 44.498036°W, 1292 m, ~50 km; (3) 63.55297°N, 52.22512°W, 519 m, ~30 km; and (4) 50.2367485°N, 45.835899°W, 3,721 m, ~1,000 km. For the filtration, 1–7 L of core-top water was siphoned into a bottle with minimal disturbance to the core, although recovery of the coring frame will have resuspended some of the core-top sediment, such that the samples reflect bottom water-suspended particles with a significant proportion of uppermost sediment particles. This sample was then pressure filtered through 142-mm quartz microfiber filters (nominal pore size 1.0 μm) in an acid-clean, plastic filter housing, using a peristaltic pump. Filters were placed in plastic holders and dried in an oven overnight at 35 °C. Oven drying overnight up to at least 50 °C has been shown not to impact Fe(II) silicate minerals in marine sediment cores (Shoenfelt et al., 2018). The sediment coming off of Greenland is physically weathered by the Greenland ice sheet (Strunk et al., 2017; Wimpenny et al., 2010) and is composed mostly of primary minerals including Fe(II) silicate minerals from the underlying Precambrian igneous and metamorphic bedrock (Petersen & Rasmussen, 1980).

The West African Margin samples were obtained from the well-characterized sediment core OC437-7 GC68 used to examine North African dust deposition through the Last Glacial Maximum (LGM; McGee et al., 2016). Samples were obtained from the gravity core collected from 19.363°N, 17.282°W, 1,396-m depth, and 75 km from the modern shoreline. Sediments were freeze-dried after sampling from the core. The dust deposited to this core is primarily from the Saharan dust plume (McGee et al., 2016), containing mostly quartz and oxidized secondary minerals such as Fe oxyhydroxides and clays (Caquineau et al., 2002; Rodriguez-Navarro et al., 2018; Schroth et al., 2009; Sunda et al., 2005). North African dust is highly uniform in mineral composition, and clay-mineral-rich, indicating that it is highly chemically weathered as a whole (Prospero, 1999).

The North Pacific samples are from ODP 1208 (36.127°N, 158.2016°E, depth = 3,346 m; Bralower et al., 2002), dated 2,686.6, 2,608.1, 3,875.1, and 4,421.8 ka. Sediments were freeze-dried after sampling from the core. This core location has been shown to be impacted primarily by East Asian dust (McGee et al., 2016). Much of the sediment in East Asian deserts and the Loess Plateau is originally derived from physical weathering processes (Lu et al., 2017; Sun, 2002). A major source of East Asian dust reaching the remote (non-coastal) North Pacific ocean is thought to be Taklimakan Desert/Tarim Basin dust that is entrained in the westerlies at high elevations (>5,000 m; Sun, 2002). Desert dunes in the Taklimakan Desert are rich in fresh Fe minerals mobilized from surrounding mountains (Lu et al., 2017) through a variety of physical weathering processes that are faster with steep mountain slopes, including glacial grinding, frost weathering, salt weathering, eolian abrasion, and fluvial weathering (Sun, 2002). The presumed sources of dust to the Loess Plateau (the Gobi in Southern Mongolia and the adjoining Chinese deserts) are described as holding areas for dust rather than dust producers, and mountain processes are responsible for the initial sediment

formation (Sun, 2002). Thus, East Asian dust as a whole is impacted by low chemical weathering due to widespread aridity over at least the last 22 million years (Guo et al., 2002) and by high physical weathering processes (Sun, 2002) due to the mountain building that began ~55 million years ago (Wang et al., 2012).

The subantarctic South Atlantic and South Pacific cores are well characterized (Anderson et al., 2014; Lamy et al., 2014; Martínez-García et al., 2014) and have been studied previously to reconstruct Southern Ocean dust-borne Fe speciation over the last glacial cycle (Shoenfelt et al., 2018). The South Atlantic core is TN057-06 (42.91°S, 8.9°E, 3,751-m water depth, the site survey core for ODP 1090; Gersonde et al., 1999), and the South Pacific core is PS75/56-1 (55.16°S, 114.79°W, 3,581-m water depth). Sediments were freeze-dried after sampling from the core. We compare published XAS data from these Southern Ocean cores with new spectroscopy data for the Greenland, West African Margin, and North Pacific sediments. The dust reaching the South Atlantic and South Pacific dust fluxes is dominantly from glaciated regions, including Patagonia, Australia, and New Zealand (Lamy et al., 2014; Martínez-García et al., 2014; Shoenfelt et al., 2018).

2.2. X-Ray Absorption Spectroscopy

Collection and analysis of Fe speciation data followed published methods (Manceau et al., 2014; Newville, 2013; Shoenfelt et al., 2017; Shoenfelt et al., 2018). Details are provided in Text S1.

3. Results and Discussion

3.1. Contrasting the Dust-Borne Fe Speciation and Bioavailability of Major Dust Regions Globally

To determine the impact of local geology and weathering on dust-borne Fe mineralogy through glacial-interglacial cycles, we contrast the $Fe(II)/Fe_{total}$ and Fe mineralogy of published Southern Ocean time series (Shoenfelt et al., 2018) with that of a new time series for Saharan dust deposited to the West African Margin, which represents a low-latitude and low-elevation region without significant physical weathering processes (Table 1). The $Fe(II)/Fe_{total}$ and Fe mineralogy is determined using the XANES spectra (Figures 1a and 1b) compared to standards (Figure S2). To investigate the role of physical weathering on Fe(II) silicate content of major dust and sediment sources globally, we contrast the Fe(II) silicate contributions to $Fe(II)/Fe_{total}$ of the published Southern Ocean glacial data with that of physical-weathering-impacted East Asian dust and Greenland sediment samples (Table 1; Figures 1b–1d).

We reconstruct the $Fe(II)/Fe_{total}$ and mineral composition of low-latitude Saharan dust-borne Fe reaching the West African Margin over the last 25,000 years (Figure S3) to span Holocene (interglacial) to LGM (glacial) sediments. The $Fe(II)/Fe_{total}$ observed in the West African Margin sediments increases from ~0% in the interglacial period to ~20% during the glacial period (Table 1 and Figure S3), which means there is lower glacial $Fe(II)/Fe_{total}$ in the West African Margin cores compared to those in the Southern Ocean (Table 1). Most importantly, the Fe(II) mineral composition of the West African Margin core is different from those in the Southern Ocean, suggesting a different explanation for the changes in Fe(II) content, as we would expect from regions with different weathering regimes. Linear combination fitting of the XANES spectra with standards suggests that the $Fe(II)/Fe_{total}$ changes are dominated by pyrite for the West African Margin core (Table 1 and Figure S3). Pyrite is an authigenic mineral that forms in sediments under reducing conditions (Raiswell & Canfield, 1998). In contrast, the Fe(II) in the Southern Ocean cores is almost entirely Fe(II) silicates derived from physical weathering of bedrock by glaciers (Shoenfelt et al., 2018). Primary Fe(II) silicate content in the West African Margin core is limited or insignificant (typically <3%, the approximate level of detection) and does not change systematically with dust flux and climate as it does in the Southern Ocean (Shoenfelt et al., 2018). The highest primary Fe(II) silicate contribution to the West African Margin core is ~8% and occurs at 25,000 years at the LGM (Figure S3). This ~8% primary Fe(II) silicate contribution is more comparable to the low primary Fe(II) content of interglacial dust than the high primary Fe(II) content of glacial dust observed at high latitudes (Shoenfelt et al., 2018). The pyrite content in the West African Margin core is generally higher with higher fluxes of organic carbon and Fe to the sediments, which is consistent with the ideal conditions of pyrite formation: when increased fluxes of nutrients enhance primary production and organic carbon burial, the organic carbon decomposes to produce anoxic conditions and high dissolved Fe (Raiswell & Canfield, 1998). Pyrite is not observed in Southern Ocean sediments (Shoenfelt et al., 2018), likely due to ~10× lower carbon fluxes in the subantarctic Southern Ocean (Anderson et al., 2014) compared to the productive, coastal West African Margin core (Bradtmiller et al.,

Table 1
Global Contributions of Primary Fe(II) Silicates and Pyrite to Fe(II)/Fe$_{total}$

Regions with a time series across the last glacial period	Holocene Fe (II)/Fe$_{total}$	LGM Fe (II)/Fe$_{total}$	Contribution of primary Fe(II) silicates to Fe(II)/Fe$_{total}$	Contribution of pyrite to Fe(II)/Fe$_{total}$	Citation
Southern Ocean	~0–5%	~30–40%	up to 100%	~0–5%	Shoenfelt et al., 2018
West African Margin	~0%	~20%	~0–40%	~60–100%	This paper
Regions impacted by physical weathering (in addition to the Southern Ocean)	**Age**	**Fe(II)/Fe$_{total}$**	**Contribution of primary Fe(II) silicates to Fe(II)/Fe$_{total}$**	**Contribution of pyrite to Fe(II)/Fe$_{total}$**	**Citation**
Greenland	core tops	~35–80%	~90–100%	~0%	This paper
North Pacific	~2.7–4.4 ma	~20–30%	~80–100%	~0%	This paper

2016). Studies of Saharan dust sources suggest that the chemical weathering environment and resulting mineralogy varies across space and time (Shi et al., 2011; Shi et al., 2012), which agrees with our observation of small mineralogical changes in dust reaching the West African Margin core over the last 25,000 years. Studies that use both water and acid extraction methods as the bioavailable Fe proxy show that the bioavailable Fe fraction is lower in low-latitude desert dusts than in physically weathered glacial sources (Hawkings et al., 2018; Schroth et al., 2009). This observation supports our hypothesis that the degree of physical weathering relative to chemical weathering controls the bioavailability of dust sources globally.

The West African Margin samples suggest Fe(II) silicates are not prevalent in Saharan dust—the largest dust source at low latitudes—since physical weathering in the region is low due to its lack of glacial activity and

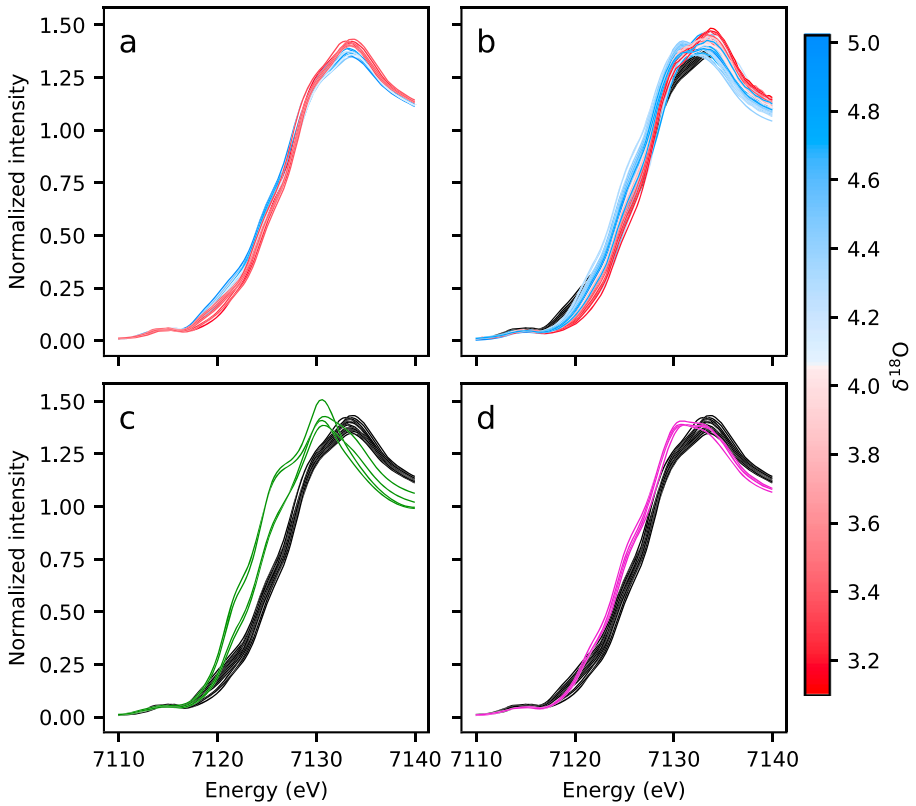

Figure 1. Iron K-edge absorption spectra for (a) a West African Margin core, (b) published Southern Ocean cores, (c) Greenland core top samples, and (d) a North Pacific core. The West African Margin samples are plotted in black for reference in b, c, and d. The colors of the spectra spanning the last glacial cycle (for (a) West African Margin and (b) Southern Ocean cores) correspond to the $\delta^{18}O$ values at the time of deposition (blues = cold glacial periods, reds = warm interglacial periods).

its generally low elevation. To confirm the role of physical weathering processes on Fe(II) silicate content of other major dust and sediment sources globally, we show that the Fe(II) silicate contributions to total Fe content of physical-weathering-impacted East Asian dust and Greenland sediment samples are comparable to and higher than that deposited to the Southern Ocean during glacial periods. These primary Fe(II) silicates are indicated by the absorption edge shifted to a lower energy, and a maximum intensity around 7,130 eV rather than 7,133 eV (Shoenfelt et al., 2017; Shoenfelt et al., 2018). The Greenland core top samples have the highest Fe(II) silicate composition and thus exhibit the strongest Fe(II) silicate features, namely, the strong shoulder and double peaks characteristic of biotite and hornblende and other primary Fe(II) silicate minerals (see Figure S2). Greenland core top samples contain ~35–80% Fe(II)/Fe_{total} with ~35–70% of total Fe attributed to biotite, hornblende, and olivine as representative primary Fe(II) silicates, and East Asian dust in North Pacific samples contains ~20–30% Fe(II)/Fe_{total} with ~20–25% of total Fe attributed to the same representative primary Fe(II) silicates (Table 1). Our observation that Fe(II) silicates are preserved in the old (2.6-4.4 ma) North Pacific sediments suggests they can be used as a proxy for particulate Fe bioavailability and physical weathering conditions on much longer time scales than attempted previously (Shoenfelt et al., 2018). Our results suggest physical weathering impacts Fe(II) silicate content of dusts in many dust source areas, including regions with glaciers (e.g., Greenland and Patagonia) and steep mountain regions (e.g., East Asia).

Our results can be summarized into two key observations: (1) Saharan dust reaching the West African Margin does not show evidence of variation in Fe(II) silicate flux on glacial-interglacial time scales, and (2) dust from East Asia and sediment from Greenland contains primary Fe(II) silicates on par with and higher than glacial Southern Ocean dust. Both of these observations suggest that physical weathering of bedrock controls the primary Fe(II) silicate content and bioavailability of Fe in dust and sediment. Published Fe speciation measurements of modern dust collected at the source corroborate our dust-borne Fe speciation reconstructions in our marine sediment cores. For the Southern Ocean, glaciogenic dust sources from Patagonia contain more primary Fe(II) silicates than nonglaciogenic sources, due to physical weathering of bedrock by glaciers (Shoenfelt et al., 2017). Northern Hemisphere glacial sources also contain high Fe (II)/Fe_{total} (>70%) contained mainly in primary Fe(II) silicates such as biotite and hornblende (Schroth et al., 2009). Additionally, poorly chemically weathered primary minerals are known to dominate the clay-size fraction of polar marine sediment (Ehrmann et al., 1992; Griffin et al., 1968; Winkler et al., 2002), supporting our observation that primary Fe(II) silicates are plentiful in physically weathered sediment reaching the ocean. East Asian dust (Chinese loess) contains 33% Fe(II)/Fe_{total} with contributions from hornblende (Schroth et al., 2009), and others have used sequential Fe extractions to suggest that East Asian dust contains fresh Fe minerals resulting from sustained and rapid erosion rates in mountain regions to the West (Lu et al., 2017). In contrast, Saharan dust sources contain 0% Fe(II)/Fe_{total} and no Fe (II) silicates (Schroth et al., 2009). Since ~80–100% of Fe in the West African Margin sediment is described by the Fe(III)-rich secondary clay glauconite rather than Fe(III) oxyhydroxides, it is likely that Fe(III) oxyhydroxides prevalent in Saharan dust (Schroth et al., 2009) have reacted with sulfides to form pyrite or have been incorporated into secondary clays. This is consistent with the observation that Fe(III) oxyhydroxides are the most reactive Fe species in the presence of sulfides in pore waters (Canfield et al., 1992), and the observation that dissolved Fe can be sequestered in glauconite as well as pyrite during sediment diagenesis (Baldermann et al., 2015). These published results suggest it is unlikely that diagenesis in the West African Margin core is responsible for the lack of primary Fe(II) silicates observed in the core samples and provide further evidence that physical weathering controls dust-borne Fe speciation and bioavailability. Thus, dust-borne Fe species observed in marine sediment cores and modern dust suggest that physical weathering controls the bioavailability of the Fe across the globe and across geologic time, through highly bioavailable primary Fe(II) silicates.

3.2. Mineralogical Continuum Between Physically and Chemically Weathered Fe in Sediments

We use PCA with all XAS samples in the XANES region (from Figure 1) as well as the standards (Figure S2) to show how physical and chemical weathering regimes impact Fe mineralogy (Figure 2). Figure S4 plots the first three principal components for our samples and standards. For XAS data analyzed with PCA, the first principal component (PC1) generally represents the most common features in Fe K-edge spectral data, including an average absorption edge (Shoenfelt et al., 2017). The second principal component (PC2) then

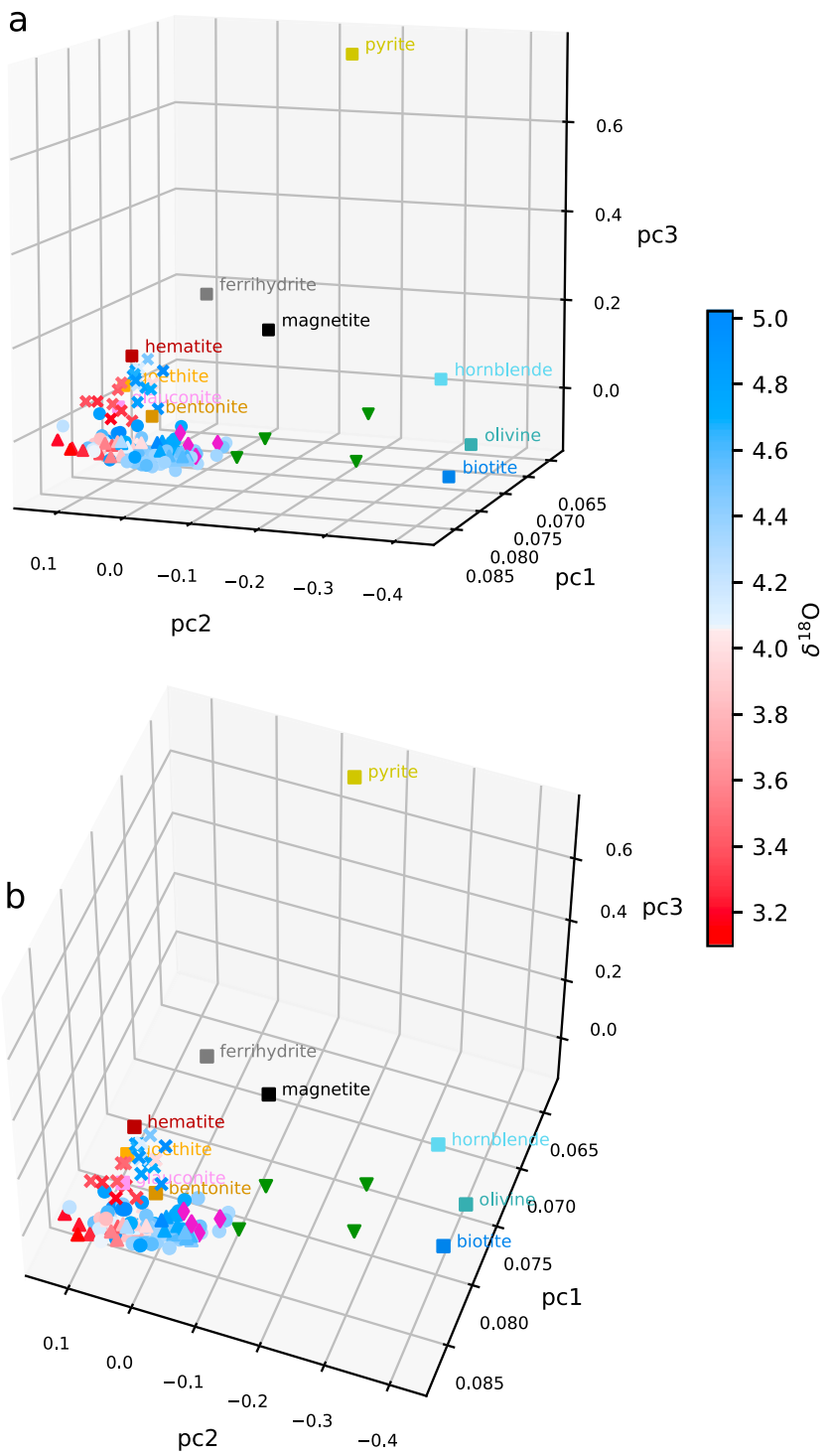

Figure 2. Loadings for the first three principal components constructed from XANES for all cores and standards. West African Margin samples are ×'s, and published South Atlantic and South Pacific samples are circles and upward triangles, respectively. West African Margin, South Atlantic, and South Pacific samples are colored by age/temperature in the same way as Figure 1 (reds = warm interglacial periods; blues = cold glacial periods). North Pacific core samples are purple diamonds, and Greenland core top samples are green downward triangles. Standards are labeled squares that are the same colors as in Figure S2. (a and b) Rotations of the same 3-D plot, for clarity. The principal components and contributions to variance are plotted in the supporting information (Figures S4 and S5).

captures the most common difference among spectra: changes in oxidation state, that is, $Fe(II)/Fe_{total}$ (Shoenfelt et al., 2017). The third principal component (PC3) represents the pyrite edge that occurs at a very low energy relative to other Fe minerals (Figure S2), suggesting that a pyrite feature is the third most common difference among spectra.

When we consider the first three principal components of the data, which explain 99.9% of the variance, we see that the low-latitude West African Margin samples cluster separately from the samples that are more heavily impacted by physical weathering and have evidence of high primary Fe(II) silicates (Figure 2). The subantarctic Southern Ocean samples vary on a continuum broadly extending from (1) Fe(III) oxide and secondary clay standards (glauconite, bentonite, goethite, and hematite) with positive PC2 loadings in interglacial periods to (2) reduced primary Fe(II) silicate standards (biotite, hornblende, and olivine) with negative PC2 loadings in glacial periods. These results suggest that physically weathered primary Fe(II) silicate content drives the glacial-interglacial differences. East Asian samples are grouped among glacial Southern Ocean samples, and Greenland samples are furthest toward the Fe(II) silicate standards. The fact that all of the Fe(II) silicates are represented well by a single component (PC2) indicates that they vary consistently and together and thus represent a relatively consistent source composed of a mixture of primary silicates, likely through physical weathering of a generally primary-mineral-rich bedrock. Notably, the sediments from the Southern Atlantic and Pacific have low PC3 loadings, suggesting that the pyrite content is low in these sediments. We expect low terrestrial pyrite in marine sediments, because pyrite quickly chemically weathers into potentially bioavailable Fe nanoparticles (Hawkings et al., 2014; Raiswell, 2011). The lack of pyrite also suggests that authigenic process are slow, likely due to relatively low organic carbon fluxes to those cores compared to the West African margin sediments. Bioavailable Fe contributions from terrestrial pyrite oxidation need to be considered when balancing Fe budgets and quantifying total Fe fluxes (Hawkings et al., 2014; Raiswell, 2011), but they generally correlate with primary Fe(II) silicate content in glaciogenic dust sources since they are also sourced from bedrock (Raiswell, 2011; Shoenfelt et al., 2017). Thus, loss of reactive Fe does not impact the use of Fe(II) silicates as a proxy for bioavailable physically weathered Fe reaching the ocean; Fe in pyrite and on reactive Fe(II) silicate surfaces is readily mobilized and likely becomes bioavailable to phytoplankton (Raiswell et al., 2018), but a primary Fe(II) silicate signature remains.

The low-latitude samples vary on a continuum from the oxidized Fe(III) standards to the Fe(II) pyrite, varying little in PC2, indicating that they do not have a significant physically weathered sediment source. These low-latitude samples instead vary most significantly in Principal Component 3 (PC3). Since pyrite has a high PC3 loading and is present only in highly productive glacial West African Margin sediments, PC3 can thus be associated with sediment authigenesis. Thus, these low-latitude sediments from the West African margin show no evidence of glaciation but instead have some evidence of increased authigenic mineral formation. These principal component data (Figure 2) thus indicate that physical weathering, and primary Fe(II) silicate content dominates differences in dust-borne Fe speciation and bioavailability among global dust sources. The data also suggest that dust sources not impacted by rapid physical weathering, such as Saharan dust, contain Fe mineral components that are produced through chemical weathering (for example Fe oxides) or diagenesis.

3.3. The Climate Implications of Physical Weathering Controlling Primary Fe(II) Silicate Content and Bioavailability of Dust-Borne Fe

The role of physical weathering on the primary Fe(II) silicate content of dust-borne Fe has both biotic and abiotic climate implications. Biotically, recent literature suggests particulate dust-borne Fe is increasingly important to phytoplankton across the world's oceans (Hawkings et al., 2018; Rubin et al., 2011; Shoenfelt et al., 2017) and may be responsible for Fe fertilization of the Southern Ocean (Shoenfelt et al., 2018). We show here that the primary Fe(II) silicate content in marine sediment cores is a consistent proxy for bioavailable physically weathered Fe reaching the ocean at a given time. Abiotically, physical weathering impacts the silicate-carbonate cycle, in which the chemical weathering of silicate minerals on land and the subsequent precipitation of carbonates in the ocean draws down atmospheric CO_2 (Raymo, 1991). The primary mineral content of sediments reaching the ocean may impact our understanding of this cycle.

We show that, globally, high physical weathering is associated with more primary Fe(II) silicates reaching the ocean. Marine sediment Fe(II) silicate records over long time scales can be combined with other

weathering proxies to determine the relative contributions of physical versus chemical weathering to the abiotic silicate-carbonate cycle (Li & Elderfield, 2013). With weak physical weathering, soil cover limits chemical weathering, and thus, the rate of physical weathering controls the overall weathering rate and the abiotic drawdown of CO_2. In contrast, when high physical weathering exposes plenty of fresh, unweathered rock fragments, the kinetics of chemical weathering controls the overall weathering rate and the abiotic drawdown of CO_2. We observe that strong physical weathering causes some unaltered primary Fe(II) silicates to bypass all chemical weathering, as observed in regions of high physical weathering such as those impacted by glaciers. The importance of these unaltered silicates bypassing the abiotic silicate-carbonate cycle should be explored. Instead of contributing to abiotic CO_2 drawdown, these unaltered silicates may contribute to biotic CO_2 drawdown. We would expect more Fe fertilization of phytoplankton with high physical weathering, since a fraction of those labile Fe(II) silicates likely become bioavailable to phytoplankton in the water column, through mechanisms that are still under exploration (Shoenfelt et al., 2017).

Physical weathering generally increases the labile primary Fe(II) silicate content of sediments that is associated with phytoplankton fertilization (Shoenfelt et al., 2017; Shoenfelt et al., 2018), suggesting that glaciers and mountain building increase the bioavailability of Fe in a given sediment flux. Since we associate enhanced physical weathering with high bioavailability of Fe(II) silicates, and physical weathering increases with high slopes and Alpine glaciers (Herman et al., 2015), it is likely that mountain building triggers both biotic drawdown of CO_2 through Fe fertilization and the abiotic drawdown of CO_2 through silicate weathering. The relative impact of these two phenomena must be quantified robustly and will depend on the time scales under consideration, since biotic CO_2 drawdown impacts atmospheric CO_2 and climate much faster than abiotic drawdown: millennia (Martínez-García et al., 2014) versus tens of millions of years (Raymo, 1991). It is possible that the physically weathered dust-borne primary Fe(II) silicates that bypass the abiotic silicate-carbonate cycle and have the chance to fertilize phytoplankton may impact our understanding of the impact of mountain building on climate change and the balance between the biotic and abiotic carbon cycle.

Acknowledgments
Thank you to David McGee for providing the freeze-dried West African Margin samples. The Greenland samples were collected during expedition DY081 funded by the European Research Council (Grant Agreement ERC-2015-StG-678371 ICY-LAB). Use of the Stanford Synchrotron Radiation Lightsource, SLAC National Accelerator Laboratory, is supported by the U.S. Department of Energy, Office of Science, Office of Basic Energy Sciences under Contract DE-AC02-76SF00515. E. M. S. was supported during her graduate work by National Science Foundation Graduate Research Fellowship DGE 16-44869, and she is currently supported by a W. O. Crosby Postdoctoral Fellowship at the Massachusetts Institute of Technology. A. L. A. was funded by NERC Independent Research Fellowship NE/P017630/1. This work was also supported by research funding from the Lamont-Doherty Earth Observatory Climate Center. This is Lamont contribution number 8354. The data supporting the conclusions is deposited in Harvard Dataverse (with the persistent URL https://doi.org/10.7910/DVN/UPTI67).

References

Anderson, R. F., Barker, S., Fleisher, M., Gersonde, R., Goldstein, S. L., Kuhn, G., et al. (2014). Biological response to millennial variability of dust and nutrient supply in the Subantarctic South Atlantic Ocean. *Philosophical Transactions of the Royal Society A*, *372*(2019). https://doi.org/10.1098/rsta.2013.0054

Anderson, S. P. (2005). Glaciers show direct linkage between erosion rate and chemical weathering fluxes. *Geomorphology*, *67*(1-2), 147–157. https://doi.org/10.1016/j.geomorph.2004.07.010

Baldermann, A., Warr, L. N., Letofsky-Papst, I., & Mavromatis, V. (2015). Substantial iron sequesteration during green-clay authigenesis in modern deep-sea sediments. *Nature Geoscience*, *8*(11), 885–889. https://doi.org/10.1038/ngeo2542

Bowen, N. L. (1922). The behavior of inclusions in igneous magmas. *Journal of Geology*, *30*(6).

Boyd, P. W., & Ellwood, M. J. (2010). The biogeochemical cycle of iron in the ocean. *Nature Geoscience*, *3*(10), 675–682. https://doi.org/10.1038/ngeo964

Bradtmiller, L. I., McGee, D., Awalt, M., Evers, J., Yerxa, H., Kinsley, C. W., & deMenocal, P. B. (2016). Changes in biological productivity along the northwest African margin over the past 20,000 years. *Paleoceanography*, *31*, 185–202. https://doi.org/10.1002/2015PA002862

Bralower, T. J., Silva, I. P., & Malone, M. J. (2002). Site 1208. *Proc. ODP, Init. Repts., 198*. https://doi.org/10.2973/odp.proc.ir.198.2002

Canfield, D. E., Raiswell, R., & Bottrell, S. (1992). The reactivity of sedimentary iron minerals toward sulfide. *American Journal of Science*, *292*(9), 659–683. https://doi.org/10.2475/ajs.292.9.659

Caquineau, S., Gaudichet, A., Gomes, L., & Legrand, M. (2002). Mineralogy of Saharan dust transported over northwestern tropical Atlantic Ocean in relation to source regions. *Journal of Geophysical Research*, *107*(D15), 4215. https://doi.org/10.1029/2000jd000247

Carmichael, I. S. E., & Ghiorso, M. S. (1986). Oxidation-reduction relations in basic magma: A case for homogenous equilibrium. *Earth and Planetary Science Letters*, *78*(2-3), 200–210. https://doi.org/10.1016/0012-821X(86)90061-0

Cornell, R. M., & Schwertmann, U. (2003). *The iron oxides: Structure, properties, reactions, occurences and uses*, (2nd ed.). Weinheim: Wiley. https://doi.org/10.1002/3527602097

Ehrmann, W. U., Melles, M., Kuhn, G., & Grobe, H. (1992). Significance of clay mineral assemblages in the Antarctic Ocean. *Marine Geology*, *107*(4), 249–273. https://doi.org/10.1016/0025-3227(92)90075-S

Gersonde, R., Hodell, D. A., & Blum, P. (1999). Proc. ODP, Init. Repts., 177.

Griffin, J. J., Windom, H., & Goldberg, E. D. (1968). The distribution of clay minerals in the World Ocean. *Deep Sea Research*, *15*, 433–459.

Guo, Z. T., Ruddiman, W. F., Hao, Q. Z., Wu, H. B., Qiao, Y. S., Zhu, R. X., et al. (2002). Onset of Asian desertification by 22 Myr ago inferred from loess deposits in China. *Nature*, *416*(6877), 159–163. https://doi.org/10.1038/416159a

Hawkings, J. R., Benning, L. G., Raiswell, R., Kaulich, B., Araki, T., Abyaneh, M., et al. (2018). Biolabile ferrous iron bearing nanoparticles in glacial sediments. *Earth and Planetary Science Letters*, *493*, 92–101. https://doi.org/10.1016/j.epsl.2018.04.022

Hawkings, J. R., Wadham, J. L., Tranter, M., Raiswell, R., Benning, L. G., Statham, P. J., et al. (2014). Ice sheets as a significant source of highly reactive nanoparticulate iron to the oceans. *Nature Communications*, *5*(1), 3929. https://doi.org/10.1038/ncomms4929

Herman, F., Beyssac, O., Brughelli, M., Lane, S. N., Leprince, S., Adatte, T., et al. (2015). Erosion by an Alpine Glacier. *Science*, *350*(6257), 193–195. https://doi.org/10.1126/science.aab2386

Kalsbeek, F. (1982). The evolution of the Precambrian Shield of Greenland. *Geologische Rundschau*, *71*(1), 38–60. https://doi.org/10.1007/BF01825023

Lam, P. J., Ohnemus, D. C., & Marcus, M. A. (2012). The speciation of marine particulate iron adjacent to active and passive continental margins. *Geochimica et Cosmochimica Acta*, *80*, 108–124. https://doi.org/10.1016/j.gca.2011.11.044

Lamy, F., Gersonde, R., Winckler, G., Esper, O., Jaeschke, A., Kuhn, G., et al. (2014). Increased dust deposition in the Pacific Southern Ocean during Glacial Periods. *Science*, *343*(6169), 403–407. https://doi.org/10.1126/science.1245424

Li, G., & Elderfield, H. (2013). Evolution of carbon cycle over the past 100 million years. *Geochimica et Cosmochimica Acta*, *103*, 11–25. https://doi.org/10.1016/j.gca.2012.10.014

Lu, W., Zhao, W., Balsam, W., Lu, H., Liu, P., Lu, Z., & Ji, J. (2017). Iron mineralogy and speciation in clay-sized fractions of chinese desert sediments. *Journal of Geophysical Research: Atmospheres*, *122*, 13,458–13,471. https://doi.org/10.1002/2017JD027733

Manceau, A., Marcus, M., & Lenoir, T. (2014). Estimating the number of pure chemical components in a mixture by X-ray absorption spectroscopy. *Journal of Synchrotron Radiation*, *21*(5), 1140–1147. https://doi.org/10.1107/S1600577514013526

Martínez-García, A., Sigman, D. M., Ren, H., Anderson, R. F., Straub, M., Hodell, D. A., et al. (2014). Iron fertilization of the Subantarctic Ocean during the last ice age. *Science*, *343*(6177), 1347–1350. https://doi.org/10.1126/science.1246848

McGee, D., Winckler, G., Borunda, A., Serno, S., Anderson, R. F., Recasens, C., et al. (2016). Tracking eolian dust with helium and thorium: Impacts of grain size and provenance. *Geochimica et Cosmochimica Acta*, *175*, 47–67. https://doi.org/10.1016/j.gca.2015.11.023

Montgomery, D. R., Balco, G., & Willett, S. D. (2001). Climate, tectonics, and the morphology of the Andes. *Geology*, *29*(7), 579–582. https://doi.org/10.1130/0091-7613(2001)029<0579:CTATMO>2.0.CO;2

Newville, M. (2013). Larch: An analysis package for XAFS and related spectroscopies. *Journal of Physics Conference Series*, *430*, 012007. https://doi.org/10.1088/1742-6596/430/1/012007

Petersen, L., & Rasmussen, K. (1980). Mineralogical composition of the clay fraction of two fluvio-glacial sediments from East Greenland. *Clay Minerals*, *15*(2), 135–145. https://doi.org/10.1180/claymin.1980.015.2.04

Polyviou, D., Baylay, A. J., Hitchcock, A., Robidart, J., Moore, C. M., & Bibby, T. S. (2018). Desert dust as a source of iron to the globally important diazotroph Trichodesmium. *Frontiers in Microbiology*, *8*(2683). https://doi.org/10.3389/fmicb.2017.02683

Prospero, J. M. (1999). Long-range transport of mineral dust in the global atmosphere: Impact of African dust on the environment of the southeastern United States. *PNAS*, *96*(7), 3396–3403. https://doi.org/10.1073/pnas.96.7.3396

Raiswell, R. (2011). Iceberg-hosted nanoparticulate Fe in the Southern Ocean: Mineralogy, origin, dissolution kinetics and source of bioavailable Fe. *Deep Sea Research, Part II*, *58*(11-12), 1364–1375. https://doi.org/10.1016/j.dsr2.2010.11.011

Raiswell, R., Benning, L. G., Tranter, M., & Tulaczyk, S. (2008). Bioavailable iron in the Southern Ocean: The significance of the iceberg conveyor belt. *Geochemical Transactions*, *9*(1). https://doi.org/10.1186/1467-4866-9-7

Raiswell, R., & Canfield, D. E. (1998). Sources of iron for pyrite formation in marine sediments. *American Journal of Science*, *298*(3), 219–245. https://doi.org/10.2475/ajs.298.3.219

Raiswell, R., Hawkings, J., Elsenousy, A., Death, R., Tranter, M., & Wadham, J. (2018). Iron in glacial systems: Speciation, reactivity, freezing behavior, and alteration during transport. *Frontiers in Earth Science*, *6*(222). https://doi.org/10.3389/feart.2018.00222

Raymo, M. E. (1991). Geochemical evidence supporting T. C. Chamberlin's theory of glaciation. *Geology*, *19*(4), 344–347. https://doi.org/10.1130/0091-7613(1991)019<0344:GESTCC>2.3.CO;2

Riebe, C. S., Kirchner, J. W., & Finkel, R. C. (2004). Erosional and climatic effects on long-term chemical weathering rates in granitic landscapes spanning diverse climate regimes. *Earth and Planetary Science Letters*, *224*(3-4), 547–562. https://doi.org/10.1016/j.epsl.2004.05.019

Rodriguez-Navarro, C., Lorenzo, F. d., & Elert, K. (2018). Mineralogy and physiochemical features of Saharan dust wet deposited in the Iberian Peninsula during an extreme red rain event. *Atmospheric Chemistry and Physics*, *18*(13), 10,089–10,122. https://doi.org/10.5194/acp-18-10089-2018

Rubin, M., Berman-Frank, I., & Shaked, Y. (2011). Dust- and mineral-iron utilization by the marine dinitrogen-fixer Trichodesmium. *Nature Geoscience*, *4*(8), 529–534. https://doi.org/10.1038/ngeo1181

Schepanksi, K. (2018). Transport of mineral dust and its impact on climate. *Geosciences*, *8*, 151.

Scher, H., & Bohaty, S. M. (2011). Two-stepping into the icehouse: East Antarctic weathering during progressive ice-sheet expansion at the Eocene-Oligocene Transition. *Geology*, *39*(4), 383–386. https://doi.org/10.1130/G31726.1

Schroth, A. W., Crusius, J., Sholkovitz, E. R., & Bostick, B. C. (2009). Iron solubility driven by speciation in dust sources to the ocean. *Nature Geoscience*, *2*(5), 337–340. https://doi.org/10.1038/ngeo501

Shi, Z., Krom, M. D., Bonneville, S., Baker, A. R., Bristow, C., Drake, N., et al. (2011). Influence of chemical weathering and aging of iron oxides on the potential iron solubility of Saharan dust during simulated atmospheric processing. *Global Biogeochemical Cycles*, *25*, GB2010. https://doi.org/10.1029/2010GB003837

Shi, Z., Krom, M. D., Jickells, T. D., Bonneville, S., Carslaw, K. S., Mihalopoulos, N., et al. (2012). Impacts on iron solubility in the mineral dust by process in the source region and the atmosphere: A review. *Aeolian Research*, *5*, 21–42. https://doi.org/10.1016/j.aeolia.2012.03.001

Shoenfelt, E. M., Sun, J., Winckler, G., Kaplan, M. R., Borunda, A. L., Farrell, K. R., et al. (2017). High particulate iron (II) content in glacially sourced dusts enhances productivity of a model diatom. *Science Advances*, *3*(6). https://doi.org/10.1126/sciadv.1700314

Shoenfelt, E. M., Winckler, G., Lamy, F., Anderson, R. F., & Bostick, B. C. (2018). Highly bioavailable dust-borne iron delivered to the Southern Ocean during glacial periods. *PNAS*, *115*(44), 11,180–11,185. https://doi.org/10.1073/pnas.1809755115

Sposito, G. (2008). *The Chemistry of Soils*. New York, New York: Oxford University Press.

Strunk, A., Knudsen, M. F., Engholm, D. L., Jansen, J. D., Levy, L. B., Jacobsen, B. H., & Larsen, N. K. (2017). One million years of glaciation and denudation history in west Greenland. *Nature Communications*, *8*(14199, 1). https://doi.org/10.1038/ncomms14199

Sun, J. (2002). Provenance of loess material and formation of loess deposits on the Chinese Loess Plateau. *Earth and Planetary Science Letters*, *203*(3-4), 845–859. https://doi.org/10.1016/S0012-821X(02)00921-4

Sunda, W. G. (2001). Bioavailability and bioaccumulation of iron in the sea. In D. R. Turner, & K. A. Hunter (Eds.), *The biogeochemistry of iron in seawater* (pp. 41–85). Chinchester, England: John Wiley & Sons.

Sunda, W. G., Price, N. M., & Morel, F. M. M. (2005). Trace metal ion buffers and their use in culture studies. In R. A. Anderson (Ed.), *Algal Culturing Techniques* (pp. 35–63). Burlington, MA, USA: Elsevier Academic Press.

von der Heyden, B. P., Roychoudhury, A. N., Mtshali, T. N., Tyliszczak, T., & Myneni, S. C. B. (2012). Chemically and geographically distinct solid-phase iron pools in the Southern Ocean. *Science*, *338*(6111), 1199–1201. https://doi.org/10.1126/science.1227504

Wang, Y., Zheng, J., Zhang, W., Li, S., Liu, X., Yang, X., & Liu, Y. (2012). Cenozoic uplift of the Tibetan Plateau: Evidence from the tectonic-sedimentary evolution of the western Qaidam Basin. *Geoscience Frontiers*, *3*(2), 175–187.

Weaver, C. E. (1990). Chapter III soils and weathering. In C. E. Weaver (Ed.), *Clays, Muds, and Shales* (Vol. *44*, pp. 103–188).
Wimpenny, J., James, R. H., Burton, K. W., Gannoun, A., Mokadem, F., & Gíslason, S. R. (2010). Glacial effects on weathering processes: New insights from the elemental and lithium isotopic composition of West Greenland rivers. *Earth and Planetary Science Letters*, *290*(3-4), 427–437. https://doi.org/10.1016/j.epsl.2009.12.042
Winkler, A., Wolf-Welling, T. C. W., Stattegger, K., & Thiede, J. (2002). Clay mineral sedimentation in high northern latitude deep-sea basins since the Middle Miocene (ODP Leg 151, NAAG). *International Journal of Earth Sciences*, *91*(1), 133–148. https://doi.org/10.1007/s005310100199